Chapter C-XV-1

Complementary Waveforms for Sidelobe Suppression and Radar Polarimetry

Yuejie Chi, Ali Pezeshki, and A. Robert Calderbank

1. Introduction

Advances in active sensing are enabled by the ability to control new degrees of freedom and each new generation of radar platforms requires fundamental advances in radar signal processing [1],[2]. The advent of phased array radars and space-time adaptive processing have given radar designers the ability to make radars adaptable on receive [2]. Modern radars are increasingly being equipped with arbitrary waveform generators which enable transmission of different waveforms across space, time, frequency, and polarization on a pulse-by-pulse basis. The design of waveforms that effectively utilize the degrees of freedom available to current and future generation of radar systems is of fundamental importance. The complexity of the design problem motivates assembly of full waveforms from a number of components with smaller time-bandwidth products and complementary properties. By choosing to separate waveforms in space, time, frequency, polarization, or a combination of these degrees of freedom, we can modularize the design problem. Modularity allows us to first analyze the effect of each control variable in isolation and then integrate across degrees of freedom (e.g., time and polarization) to enable adaptive control of the radar's operation.

Sixty years ago, efforts by Marcel Golay to improve the sensitivity of far infrared spectrometry led to the discovery of complementary sequences [3]–[5], which have the property that the sum of their autocorrelation functions vanishes at all delays other than zero. Almost a decade after their invention, Welti rediscovered complementary sequences (there are his D-codes) [6] and proposed to use them for pulsed radar. However, since then they have found very limited application in radar as it soon became evident that the perfect autocorrelation property of complementary sequences cannot be easily utilized in practice. The reason, to quote Ducoff and Tietjen [7], is "in a practical application, the two sequences must be separated in time, frequency, or polarization, which results in decorrelation of radar returns so that complete sidelobe

The research contributions presented here were supported in part by the National Science Foundation under Grant 0701226, by the Office of Naval Research under Grant N00173-06-1-G006, and by the Air Force Office of Scientific Research under Grant FA9550-05-1-0443.

Y. Chi is with the Department of Electrical Engineering, Princeton University, Princeton, NJ 08544, USA. Email: ychi@princeton.edu.

A. Pezeshki is with the Department of Electrical and Computer Engineering, Colorado State University, Fort Collins, CO 80523, USA. Email: pezeshki@engr.colostate.edu.

A. R. Calderbank is with the Program in Applied and Computational Mathematics, Princeton University, Princeton, NJ 08544, USA. Email: calderbk@math.princeton.edu.

cancellation may not occur. Hence they have not been widely used in pulse compression radars." Various generalizations of complementary sequences including multiple complementary codes by Tseng and Liu [8] and multiphase (or polyphase) complementary sequences by Sivaswami [9] and Frank [10] suffer from the same problem.

In this chapter, we present a couple of examples to demonstrate how degrees of freedom available for radar transmission can be exploited, in conjunction with the complementary property of Golay sequences, to dramatically improve target detection performance. The chapter is organized as follows. In Section 2, we describe Golay complementary waveforms and highlight the major barrier in employing them for radar pulse compression. In Section 3, we will consider coordinating the transmission of Golay complementary waveforms in time (over pulse repetition intervals) to construct *Doppler resilient pulse trains*, for which the ambiguity function is effectively free of range sidelobes inside a desired Doppler interval. This construction demonstrates the value of waveform agility in time for achieving radar ambiguity responses not possible with conventional pulse trains. The materials presented in this section are based on work reported in [11]–[13]. In Section 4, we will present a new radar primitive that enables *instantaneous radar polarimetry* at essentially no increase in signal processing complexity. In this primitive the transmission of Golay complementary waveforms is coordinated across orthogonal polarization channels and over time in an Alamouti fashion to construct a *unitary* polarization-time waveform matrix. The unitary property enables simple receive signal processing which makes the full polarization scattering matrix of a target available for detection on a pulse-by-pulse basis (instantaneously). The materials presented in this section are based on work reported in [14],[15],[11].

2. Golay Complementary Waveforms

2.1. Complementary Sequences

Definition 1: Two length L unimodular[1] sequences of complex numbers $x(\ell)$ and $y(\ell)$ are Golay complementary if for $k = -(L-1), \ldots, (L-1)$ the sum of their autocorrelation functions satisfies

$$C_x(k) + C_y(k) = 2L\delta(k) \tag{1}$$

where $C_x(k)$ is the autocorrelation of $x(\ell)$ at lag k and $\delta(k)$ is the Kronecker delta function. This property is often expressed as

$$|X(z)|^2 + |Y(z)|^2 = 2L \tag{2}$$

where $X(z)$ is the z-transform of $x(\ell)$ given by the polynomial

$$X(z) = \sum_{\ell=0}^{L-1} x(\ell) z^{-\ell}. \tag{3}$$

[1]The original complementary sequences invented by Golay for spectrometry were binary and polyphase complementary sequences were invented later. However, in this chapter we will not distinguish between them and refer to all complementary pairs as Golay complementary.

Henceforth we may drop the discrete time index ℓ from $x(\ell)$ and $y(\ell)$ and simply use x and y. Each member of the pair (x, y) is called a Golay sequence.

At first, it may appear that complementary sequences are ideal for radar pulse compression. However, as we will show in Section 2.2. the complementary property of these sequences is extremely sensitive to Doppler effect. For this reason, complementary sequences have not found wide applicability in radar, despite being discovered almost sixty years ago. Some of the early articles that explore the use of Golay complementary sequences (or their generalizations to polyphase and multiple complementary sequences) for radar are [6],[8]–[10].

2.2. Golay Complementary Waveforms for Radar

A baseband waveform $w_x(t)$ phase coded by a Golay sequence x is given by

$$w_x(t) = \sum_{\ell=0}^{L-1} x(\ell)\Omega(t - \ell T_c) \tag{4}$$

where $\Omega(t)$ is a unit energy pulse shape of duration T_c and T_c is the chip length. The ambiguity function $\chi_{w_x}(\tau, \nu)$ of $w_x(t)$ is given by

$$\begin{aligned}\chi_{w_x}(\tau, \nu) &= \int_{-\infty}^{\infty} w_x(t)\overline{w_x(t-\tau)}e^{-j\nu t}dt \\ &= \sum_{k=-(L-1)}^{L-1} A_x(k, \nu T_c)\chi_\Omega(\tau + kT_c, \nu)\end{aligned} \tag{5}$$

where $\overline{w(t)}$ is the complex conjugate of $w(t)$, $\chi_\Omega(\tau, \nu)$ is the ambiguity function of the pulse shape $\Omega(t)$, and $A_x(k, \nu T_c)$ is given by

$$A_x(k, \nu T_c) = \sum_{\ell=-(L-1)}^{L-1} x(\ell)\overline{x(\ell - k)}e^{-j\nu\ell T_c}. \tag{6}$$

If complementary waveforms $w_x(t)$ and $w_y(t)$ are transmitted separately in time, with a T sec time interval between the two transmissions, then the ambiguity function of the radar waveform $w(t) = w_x(t) + w_y(t - T)$ is given by[2]

$$\chi_w(\tau, \nu) = \chi_{w_x}(\tau, \nu) + e^{j\nu T}\chi_{w_y}(\tau, \nu). \tag{7}$$

Since the chip length T_c is typically very small, the relative Doppler shift over chip intervals is negligible compared to the relative Doppler shift over T, and the ambiguity

[2]The ambiguity function of $w(t)$ has two range aliases (cross terms) which are offset from the zero-delay axis by $\pm T$. In this chapter, we ignore the range aliasing effects and refer to $\chi_w(\tau, \nu)$ as the ambiguity function of $w(t)$. Range aliasing effects can be accounted for using standard techniques devised for this purpose (e.g. see [16]) and hence will not be further discussed.

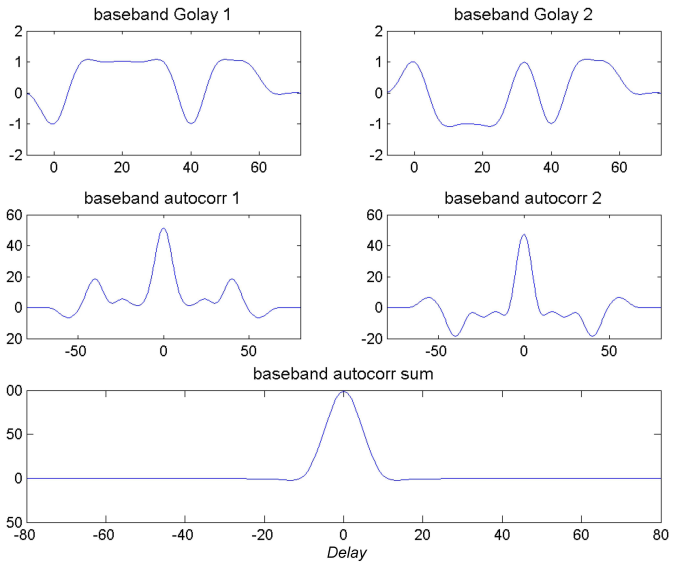

Figure 1 . The perfect autocorrelation property of a Golay pair of phase coded waveforms

function $\chi_w(\tau,\nu)$ can be approximated by

$$\chi_w(\tau,\nu) = \sum_{k=-(L-1)}^{L-1} [C_x(k) + e^{j\nu T} C_y(k)]\chi_\Omega(\tau + kT_c, \nu) \tag{8}$$

where in this approximation we have replaced $A_x(k,\nu T_c)$ and $A_y(k,\nu T_c)$ with the autocorrelation functions $C_x(k)$ and $C_y(k)$, respectively.

Along the zero-Doppler axis ($\nu = 0$), the ambiguity function $\chi_w(\tau,\nu)$ reduces to the autocorrelation sum

$$\chi_w(\tau,0) = \sum_{k=-(L-1)}^{L-1} [C_x(k) + C_y(k)]\chi_\Omega(\tau + kT_c, 0) = 2L\chi_\Omega(\tau,0) \tag{9}$$

where the second equality follows from (1). This means that along the zero-Doppler axis the ambiguity function $\chi_w(\tau,\nu)$ is "free" of range sidelobes.[3] This perfect autocorrelation property (ambiguity response along zero-Doppler axis) is illustrated in Fig. 1 for a Golay pair of phase coded waveforms.

Off the zero-Doppler axis however, the ambiguity function $\chi_w(\tau,\nu)$ has large sidelobes in delay (range) as Fig. 2 shows. The color bar values are in dB. The range side-

[3]The shape of the autocorrelation function depends on the autocorrelation function $\chi_\Omega(\tau,0)$ for the pulse shape $\Omega(t)$. The Golay complementary property eliminates range sidelobes caused by replicas of $\chi_\Omega(\tau,0)$ at nonzero integer delays.

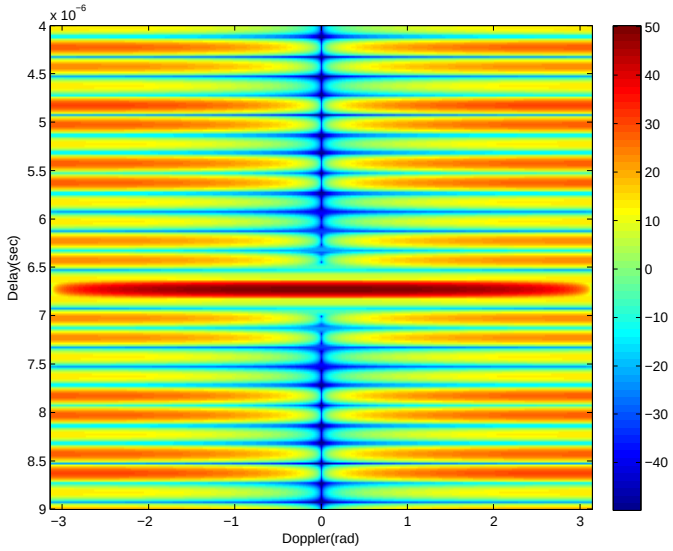

Figure 2 . The ambiguity function of a Golay pair of phase coded waveforms separated in time

lobes persist even when a pulse train is constructed in which $w(t) = w_x(t)+w_y(t-T)$ is transmitted several times, with a pulse repetition interval (PRI) of T seconds between consecutive transmissions. In other words, the ambiguity function of a conventional pulse train of Golay complementary waveforms, where the transmitter alternates between $w_x(t)$ and $w_y(t)$ during several PRIs, also has large range sidelobes along nonzero Dopplers. The presence of Doppler-induced range sidelobes in the ambiguity function means that a strong reflector can mask a nearby (in range) weak target that is moving at a different speed. Figure 3 shows the delay-Doppler map at the output of a radar receiver (matched filter), when a conventional (alternating) pulse train of Golay complementary waveforms was transmitted over 256 PRIs. The horizontal axis shows Doppler and the vertical axis depicts delay. Color bar values are in dB. The radar scene contains three stationary reflectors at different ranges and two slow-moving targets, which are 30dB weaker than the stationary reflectors. We notice that the range sidelobes from the strong stationary reflectors make it difficult to resolve the weak slow-moving targets. The sensitivity of Golay complementary waveforms to Doppler effect has been the main barrier in adopting these waveforms for radar pulse compression. As we will show in Section 3, this issue can be resolved by properly coordinating the transmission of Golay complementary waveforms over time.

3. Doppler Resilient Pulse Trains

Waveform agile radars are capable of changing their transmit waveform on a pulse-by-pulse basis, and hence are not limited to transmitting the same waveform (or wave-

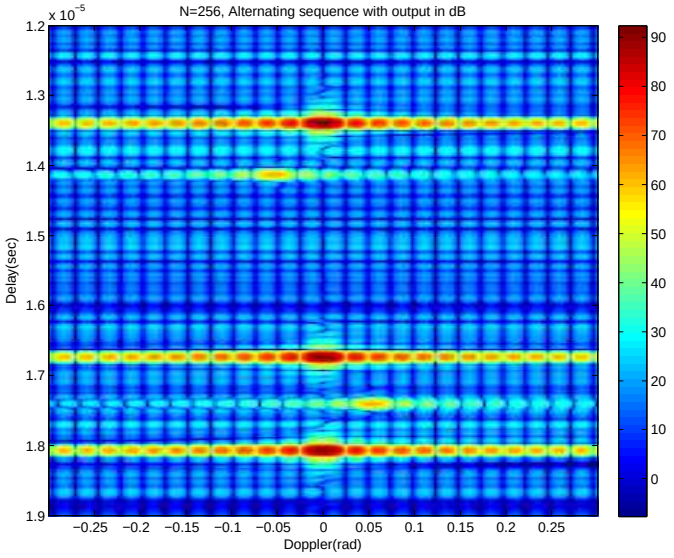

Figure 3 . Delay-Doppler map at the output of a radar receiver (matched filter), when a conventional (alternating) pulse train of Golay complementary waveforms is transmitted.

form pair) over time. It is natural to ask whether or not it is possible to exploit this new degree of freedom to construct a *Doppler resilient* pulse train (or sequence) of Golay complementary waveforms, for which the range sidelobes of the pulse train ambiguity function vanish inside a desired Doppler interval. Following the developments in [11]–[13], we show in this section that this is indeed possible and can be achieved by coordinating the transmission of a Golay pair of phase coded waveforms $(w_x(t),w_y(t))$ in time according to 1's and -1's in a properly designed biphase sequence.

Definition 2: Consider a biphase sequence $\mathcal{P} = \{p_n\}_{n=0}^{N-1}$, $p_n \in \{-1, 1\}$ of length N, where N is even. Let 1 represent $w_x(t)$ and let -1 represent $w_y(t)$. The *$\mathcal{P}$-pulse train* $w_{\mathcal{P}}(t)$ of $(w_x(t), w_y(t))$ is defined as

$$w_{\mathcal{P}}(t) = \frac{1}{2}\sum_{n=0}^{N-1}\left[(1+p_n)w_x(t-nT) + (1-p_n)w_y(t-nT)\right]. \tag{10}$$

The nth entry in $w_{\mathcal{P}}(t)$ is $w_x(t)$ if $p_n = 1$ and is $w_y(t)$ if $p_n = -1$. Consecutive entries in the pulse train are separated in time by a PRI T.

The ambiguity function of the $\mathcal{P}$-pulse train $w_{\mathcal{P}}(t)$, after ignoring the pulse shape ambiguity function and discretizing in delay (at chip intervals), can be written as [13]

$$\chi_{w_{\mathcal{P}}}(k,\theta) = \frac{1}{2}[C_x(k) + C_y(k)]\sum_{n=0}^{N-1} e^{jn\theta} + \frac{1}{2}[C_x(k) - C_y(k)]\sum_{n=0}^{N-1} p_n e^{jn\theta} \tag{11}$$

where $\theta = \nu T$ is the relative Doppler shift over a PRI. The first term on the right-hand-side of (11) is free of range sidelobes due to the complementary property of Golay sequences x and y. The second term represents the range sidelobes as $C_x(k) - C_y(k)$ is not an impulse. We notice that the magnitude of the range sidelobes is proportional to the magnitude of the spectrum $S_{\mathcal{P}}(\theta)$ of the sequence $\mathcal{P}$, which is given by

$$S_{\mathcal{P}}(\theta) = \sum_{n=0}^{N-1} p_n e^{jn\theta}. \tag{12}$$

By shaping the spectrum $S_{\mathcal{P}}(\theta)$ we can control the range sidelobes. The question is how to design the sequence $\mathcal{P}$ to suppress the range sidelobes along a desired Doppler interval. One way to accomplish this is to design $\mathcal{P}$ so that its spectrum $S_{\mathcal{P}}(\theta)$ has a high-order null at a Doppler frequency inside the desired interval.

3.1. Resilience to Modest Doppler Shifts

Let us first consider the design of a biphase sequence whose spectrum has a high-order null at zero Doppler frequency. The Taylor expansion of $S_{\mathcal{P}}(\theta)$ around $\theta = 0$ is given by

$$S_{\mathcal{P}}(\theta) = \sum_{t=0}^{\infty} \frac{1}{n!} f_{\mathcal{P}}^{(t)}(0)(\theta)^t \tag{13}$$

where the coefficients $f_{\mathcal{P}}^{(t)}(0)$ are given by

$$f_{\mathcal{P}}^{(t)}(0) = j^t \sum_{n=0}^{N-1} n^t p_n, \quad t = 0, 1, 2, \ldots \tag{14}$$

To generate an Mth-order null at $\theta = 0$, we need to zero-force all derivatives $f_{\mathcal{P}}^{(t)}(0)$ up to order M, that is, we need to design the biphase sequence $\mathcal{P}$ such that

$$\sum_{n=0}^{N-1} n^t p_n = 0, \quad t = 0, 1, 2, \ldots, M. \tag{15}$$

This is the famous Prouhet (or Prouhet-Tarry-Escott) problem [17],[18], which we now describe.

Prouhet Problem: [17],[18] Let $\mathbb{S} = \{0, 1, \ldots, N-1\}$ be the set of all integers between 0 and $N-1$. Given an integer M, is it possible to partition $\mathbb{S}$ into two disjoint subsets $\mathbb{S}_0$ and $\mathbb{S}_1$ such that

$$\sum_{r \in \mathbb{S}_0} r^m = \sum_{q \in \mathbb{S}_1} q^m \tag{16}$$

for all $0 \leq m \leq M$? Prouhet proved that this is possible only when $N = 2^{M+1}$ and that the partitions are identified by the *Prouhet-Thue-Morse sequence*.

Definition 3: [18],[19] The Prouhet-Thue-Morse (PTM) sequence $\mathcal{P} = (p_k)_{k \geq 0}$ over $\{-1, 1\}$ is defined by the following recursions:

1. $p_0 = 1$
2. $p_{2k} = p_k$
3. $p_{2k+1} = -p_k$

for all $k \geq 0$.

Theorem 1 (Prouhet) [17],[18]: Let $\mathcal{P} = (p_k)_{k\geq 0}$ be the PTM sequence. Define

$$\begin{aligned} \mathbb{S}_0 &= \{r \in \mathbb{S} = \{0, 1, 2, \ldots, 2^{M+1} - 1\} |\, p_r = 0\} \\ \mathbb{S}_1 &= \{q \in \mathbb{S} = \{0, 1, 2, \ldots, 2^{M+1} - 1\} |\, p_q = 1\} \end{aligned} \tag{17}$$

Then, (16) holds for all m, $0 \leq m \leq M$.

We have the following theorem.

Theorem 2: Let $\mathcal{P} = \{p_n\}_{n=0}^{2^M-1}$ be the length-2^M PTM sequence. Then, the spectrum $S_{\mathcal{P}}(\theta)$ of $\mathcal{P}$ has an $(M-1)$th-order null at $\theta = 0$. Consequently, the ambiguity function of a PTM pulse train of Golay complementary waveforms (transmitted over 2^M PRIs) has an $(M-1)$th-order null along the zero Doppler axis for all nonzero delays.

Example 1: The PTM sequence of length 8 is

$$\mathcal{P} = (p_k)_{k=0}^{7} \;=\; +1 \;-1 \;-1 \;+1 \;-1 \;+1 \;+1 \;-1. \tag{18}$$

The corresponding pulse train of Golay complementary waveforms is given by

$$\begin{aligned} w_{PTM}(t) \;=\; & w_x(t) + w_y(t-T) + w_y(t-2T) + w_x(t-3T) \\ & + w_y(t-4T) + w_x(t-5T) + w_x(t-6T) + w_y(t-7T). \end{aligned} \tag{19}$$

The ambiguity function of $w_{PTM}(t)$ has a second-order null along the zero-Doppler axis for all nonzero delays.

Figure 4(a) shows the ambiguity function of a length-$(N = 2^8)$ PTM pulse train of Golay complementary waveforms, which has a seventh-order null along the zero-Doppler axis. The horizonal axis is Doppler shift in rad and the vertical axis is delay in sec. The magnitude of the pulse train ambiguity function is color coded and presented in dB scale. A zoom-in around zero-Doppler is shown in Fig. 4(b). We notice that the range sidelobes inside the Doppler interval $[-0.1, 0.1]$rad have been cleared out. They are at least 80 dB below the peak of the ambiguity function. This means that a PTM pulse train can resolve a weak target that is situated in range near a strong reflector, provided that the difference in speed between the weak and strong scatterers is relatively small. Figure 5 shows the ability of the PTM pulse train in bringing out weak slow-moving targets (e.g. pedestrians) in the presence of strong stationary reflectors (e.g. buildings) for the five target scenario discussed earlier in Fig. 3. This example clearly demonstrates the value of waveform agility over time for radar imaging. We note that the Golay complementary sequences used for phase coding in obtaining Figs.

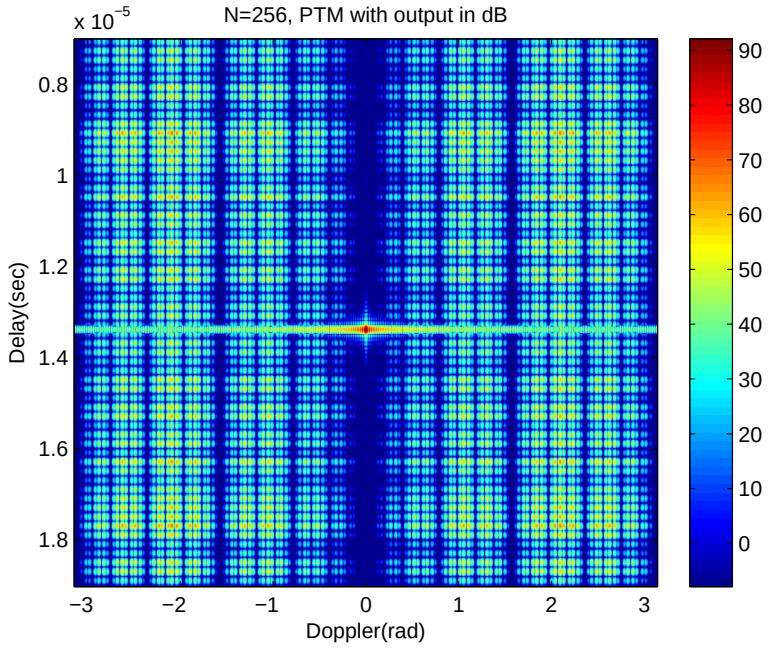

(a)

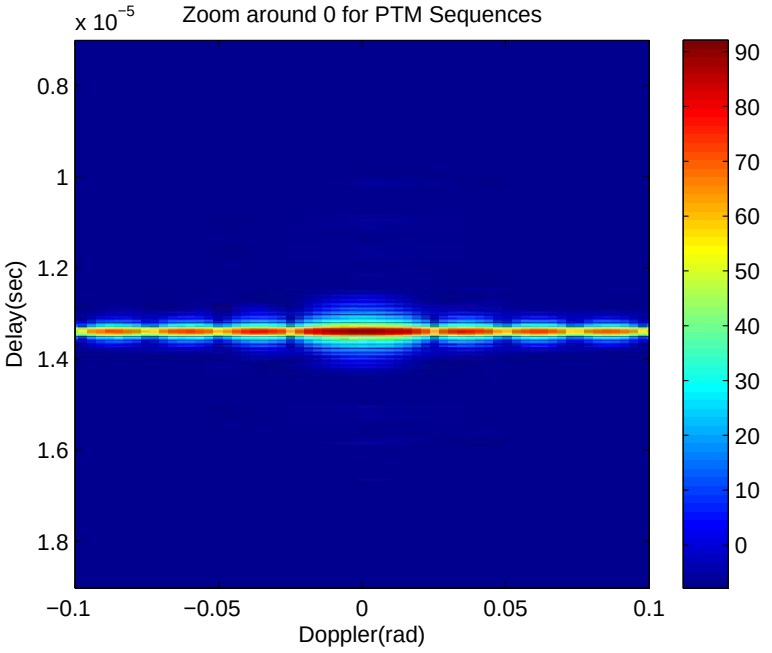

(b)

Figure 4 . Ambiguity function of a length-($N = 2^8$) PTM pulse train of Golay complementary waveforms: (a) the entire Doppler band (b) Doppler band $[-0.1, 0.1]$*rad*

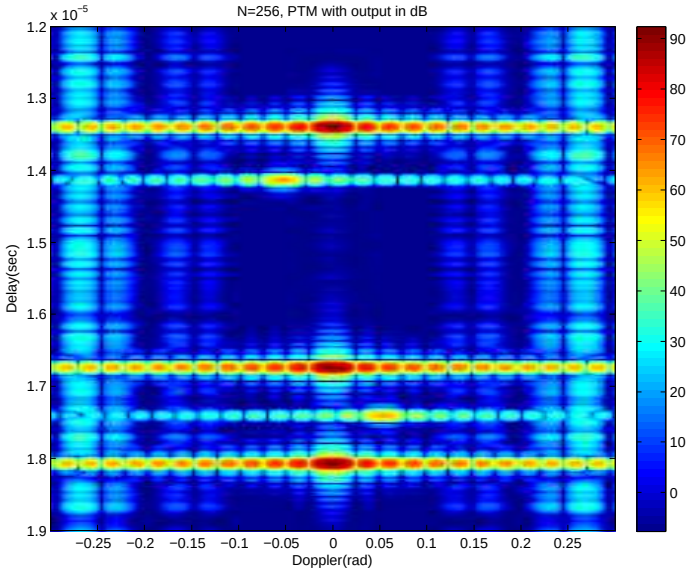

Figure 5 . The PTM pulse train of Golay complementary waveforms can bring out weak targets which would have otherwise been masked by the range sidelobes of nearby strong reflectors that move at slightly different speeds.

3–5 are of size 64 and the pulse shape is a raised cosine. The chip length is $T_c = 100$ nsec, the carrier frequency is 17 GHz, and the PRI is $T = 50$ μsec.

3.2. Resilience to Higher Doppler Frequencies

We now consider the design of biphase sequences whose spectra have high-order nulls at Doppler shifts other than zero. Consider the Taylor expansion of $S_{\mathcal{P}}(\theta)$ around $\theta = \theta_0 \neq 0$:

$$S_{\mathcal{P}}(\theta) = \sum_{t=0}^{\infty} \frac{1}{n!} f_{\mathcal{P}}^{(t)}(\theta_0)(\theta - \theta_0)^t \tag{20}$$

where the coefficients $f_{\mathcal{P}}^{(t)}(\theta_0)$ are given by

$$f_{\mathcal{P}}^{(t)}(\theta_0) = \left[\frac{d^t}{d\theta^t} S_{\mathcal{P}}(\theta)\right]_{\theta=\theta_0} = j^t \sum_{n=0}^{N-1} n^t p_n e^{jn\theta_0}, \quad t = 0, 1, 2, \ldots \tag{21}$$

We wish to zero-force all the derivatives $f_{\mathcal{P}}^{(t)}(\theta_0)$ up to order M, that is, we wish to design the sequence $\mathcal{P}$ so that

$$f_{\mathcal{P}}^{(t)}(\theta_0) = 0, \quad \text{for all } \; t = 0, 1, \ldots, M. \tag{22}$$

Here, we limit our design to rational Doppler shifts $\theta_0 = 2\pi l/m$, where l and $m \neq 1$ are co-prime integers and assume that the length of $\mathcal{P}$ is $N = mq$ for some integer q.

If we express $0 \leq n \leq N-1$ as $n = rm+i$, where $0 \leq r \leq q-1$ and $0 \leq i \leq m-1$, then using binomial expansion for $n^t = (rm+i)^t$ we can write $f_{\mathcal{P}}^{(t)}(\theta_0)$ as

$$\begin{aligned} f_{\mathcal{P}}^{(t)}(\theta_0) &= j^t \sum_{n=0}^{N-1} n^t p_n e^{jn\theta_0} && (23) \\ &= j^t \sum_{r=0}^{q-1} \sum_{i=0}^{m-1} (rm+i)^t p_{rm+i} e^{j(rm+i)\frac{2\pi l}{m}} && (24) \\ &= j^t \sum_{r=0}^{q-1} \sum_{i=0}^{m-1} \sum_{u=0}^{t} \binom{t}{u} i^{t-u} (rm)^u p_{rm+i} e^{j\frac{2\pi li}{m}} && (25) \\ &= j^t \sum_{u=0}^{t} \binom{t}{u} m^u \sum_{i=0}^{m-1} i^{t-u} e^{j\frac{2\pi li}{m}} \left[\sum_{r=0}^{q-1} r^u p_{rm+i} \right] && (26) \end{aligned}$$

Define a length-q sequence $\{b_r\}_{r=0}^{q-1}$ as $b_r = p_{rm+i},\ 0 \leq r \leq q-1$. If $\{b_r\}_{r=0}^{q-1}$ satisfies

$$\sum_{r=0}^{q-1} r^u b_r = 0, \quad \text{for all } 0 \leq u < t \tag{27}$$

then the coefficient $f_{\mathcal{P}}^{(t)}(\theta_0)$ will be zero. From Theorem 1, it follows that the zero-forcing condition in (27) will be satisfied if $\{b_r\}_{r=0}^{q-1}$ is the PTM sequence of length 2^t. We note that $f_{\mathcal{P}}^{(M)}(\theta_0)$ is automatically zero as $\sum_{i=0}^{m-1} e^{j\frac{2\pi li}{m}} = 0$. Therefore, to zero-force the derivatives $f_{\mathcal{P}}^{(t)}(\theta_0)$ for all $t \leq M$, it is sufficient to select $\mathcal{P} = \{p_n\}_{n=0}^{2^M m-1}$ such that each $\{p_{rm+i}\}_{r=0}^{q-1}$, $i = 0, \cdots, m-1$ is the length-2^M PTM sequence. We call such a sequence a $(2^M, m)$-*PTM sequence*. The $(2^M, m)$-PTM sequence has length $2^M \times m$ and is constructed from the length-2^M PTM sequence by repeating each 1 and -1 in the PTM sequence m times, that is, it is constructed by oversampling the PTM sequence by a factor m.

We have the following theorem.

Theorem 3: Let $\mathcal{P} = \{p_n\}_{n=0}^{2^M m-1}$ be the $(2^M, m)$-PTM sequence, that is to say each of $\{p_{rm+i}\}_{r=0}^{2^M-1}$, $i = 0, \cdots, m-1$ is a PTM sequence of length 2^M. Then the spectrum $S_{\mathcal{P}}(\theta)$ of $\mathcal{P}$ has Mth-order nulls at all $\theta_0 = 2\pi l/m$ where l and $m \neq 1$ are co-prime integers.

Corollary 1: Let $\mathcal{P}$ be the $(2^M, m)$-PTM sequence. Then the spectrum $S_{\mathcal{P}}(\theta)$ of $\mathcal{P}$ has an $(M-1)$th-order null at $\theta_0 = 0$ and $(M-h-1)$th-order nulls at all $\theta_0 = 2\pi l/(2^h m)$, where l and $m \neq 1$ are co-prime, and $1 \leq h \leq M-1$.

Proof: The proof for $\theta_0 = 0$ is straightforward. For $\theta_0 = 2\pi l/(2^h m)$, we have

$$f_{\mathcal{P}}^{(t)}(\theta_0) = \sum_{u=0}^{t} \binom{t}{u} (2^h m)^u \sum_{i=0}^{2^h m-1} i^{t-u} e^{j\frac{2\pi li}{2^h m}} \left[\sum_{r=0}^{\frac{q}{2^h}-1} r^u p_{2^h mr+i} \right] \tag{28}$$

where $q = 2^M$. The corollary follows from the fact that downsampling a PTM sequence by a power of 2 produces a PTM sequence of shorter length.

Theorem 3 and Corollary 1 imply that oversampled PTM pulse trains can bring out weak targets which are situated in range near strong reflectors, provided that the relative distance in Doppler shift between the weak and strong scatterers is approximately $2\pi l/(2^h m)$, where l and $m \neq 1$ are co-prime, and $1 \leq h \leq M-1$.

Example 2: The spectrum of the $(2^3, 2)$-PTM sequence

$$\mathcal{P} = \{+1, +1, -1, -1, -1, -1, +1, +1, -1, -1, +1, +1, +1, +1, -1, -1\}$$

has a third-order null at $\theta_0 = \pi$ rad, a second-order null at $\theta_0 = 0$ rad, first-order nulls at $\theta_0 = \pi/2$ rad and $\theta_0 = 3\pi/2$ rad, and zeroth-order nulls at $\theta_0 = (2k+1)\pi/4$ rad for $k = 0, 1, 2, 3$. This spectrum is shown in Fig. 6 in solid black line. The spectrum of the $(2^2, 2)$-PTM sequence is also shown in this figure in dashed black line. This spectrum has a second-order null at $\theta_0 = \pi$ rad, a first-order null at $\theta_0 = 0$ rad, and zeroth-order nulls at $\theta_0 = \pi/2$ rad and $\theta_0 = 3\pi/2$ rad.

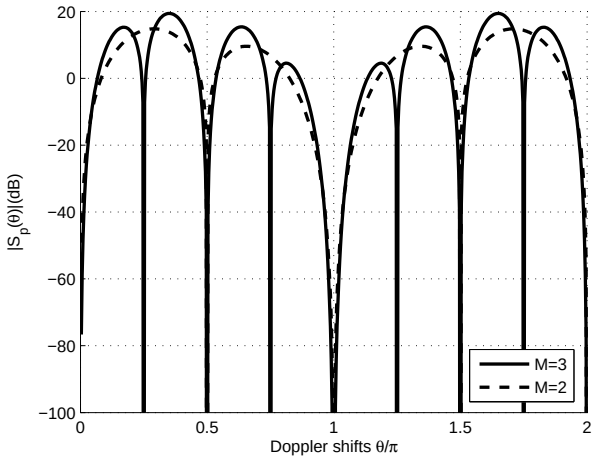

Figure 6 . The spectra of $(2^3, 2)$*- and* $(2^2, 2)$*-PTM sequences.*

Figure 7(a) shows the ambiguity function of a $(2^8, 3)$-PTM sequence of Golay complementary waveforms. The color bar values are in dB. This ambiguity function has an eighth-order null at $\theta_0 = \pm 2\pi/3$, a seventh-order null at zero Doppler, sixth-order nulls at $\theta_0 = \pm\pi/3$, and so on. A zoom in around $\theta_0 = 2\pi/3$ is provided in Fig. 7(b) to demonstrate that range sidelobes in this Doppler region are significantly suppressed. The range sidelobes in this region are at least 80 dB below the peak of the ambiguity function. This example shows the value of properly coordinating the transmission of complementary waveforms over time for achieving a desired ambiguity response.

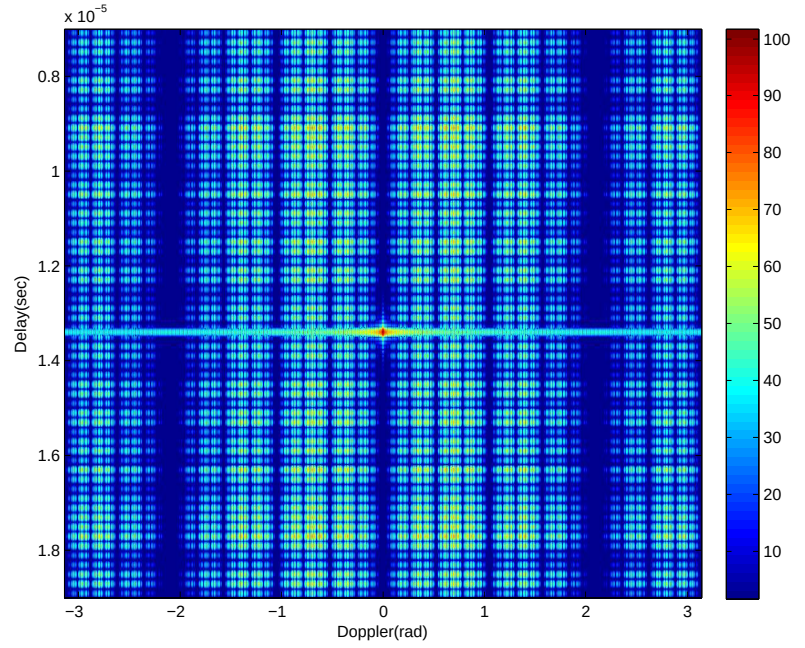

(a)

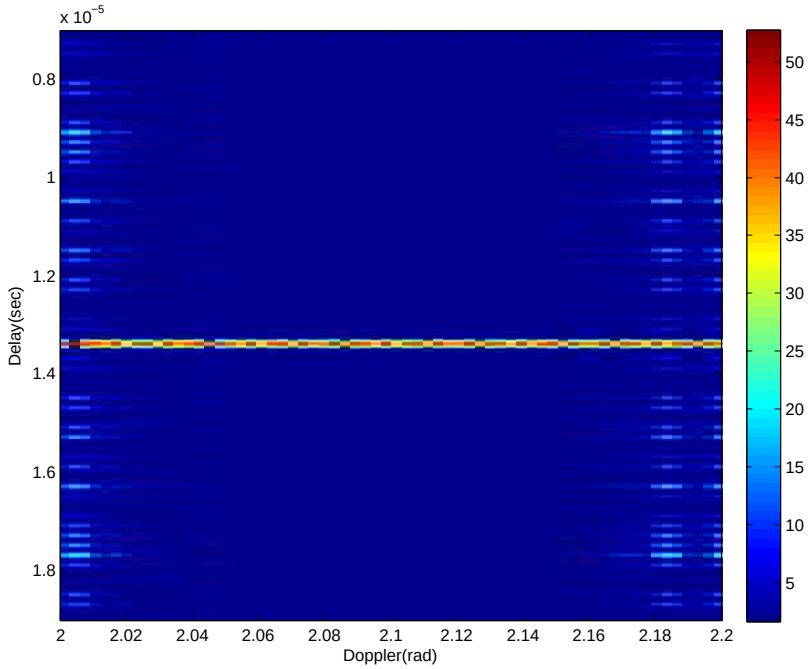

(b)

Figure 7 . Ambiguity function of the $(2^8, 3)$*-PTM pulse train of Golay complementary waveforms: (a) the entire Doppler band (b) Zoom in around* $\theta_0 = 2\pi/3$.

4. Instantaneous Radar Polarimetry

Fully polarimetric radar systems are capable of transmitting and receiving on two orthogonal polarizations simultaneously. The combined signal then has an electric field vector that is modulated both in direction and amplitude by the waveforms on the two polarization channels, and the receiver is used to obtain both polarization components of the reflected waveform. The use of two orthogonal polarizations increases the degrees of freedom available for target detection and can result in significant improvement in detection performance.

The radar cross section of an extended target such as an aircraft or a ship is highly sensitive to the angle of incidence and angle of view of the sensor (see [20] Sections 2.7–8). In general the reflection properties that apply to each polarization component are also different, and indeed reflection can change the direction of polarization. Thus, polarimetric radars are able to obtain the scattering tensor of a target

$$\mathbf{\Sigma} = \begin{pmatrix} \sigma_{VV} & \sigma_{VH} \\ \sigma_{HV} & \sigma_{HH} \end{pmatrix}, \tag{29}$$

where σ_{VH} denotes the target scattering coefficient into the vertical polarization channel due to a horizontally polarized incident field. Target detection is enhanced by concurrent rather than serial access to the cross-polarization components of the scattering tensor, which varies more rapidly in standard radar models used in target detection and tracking [21] than in models used in remote sensing or synthetic aperture radar [22],[23]. In fact what is measured is the combination of three matrices

$$\mathbf{H} = \begin{pmatrix} h_{VV} & h_{VH} \\ h_{HV} & h_{HH} \end{pmatrix} = \mathbf{C}_{\text{Rx}} \mathbf{\Sigma} \mathbf{C}_{\text{Tx}}, \tag{30}$$

where C_{Rx} and C_{Tx} correspond to the polarization coupling properties of the transmit and receive antennas, whereas $\mathbf{\Sigma}$ results from the target. In most radar systems the transmit and receive antennas are common, and so the matrices C_{Tx} and C_{Rx} are conjugate. The cross-coupling terms in the antenna polarization matrices are clearly frequency and antenna geometry dependent but for the linearly polarized case this value is typically no better than about -20dB.

In this section, we follow [14],[15] to describe a new approach to radar polarimetry that uses orthogonal polarization modes to provide essentially independent channels for viewing a target, and achieve diversity gain. Unlike conventional radar polarimetry, where polarized waveforms are transmitted sequentially and processed noncoherently, the approach in [14],[15] allows for *instantaneous radar polarimetry (IRP)*, where polarization modes are combined coherently on a pulse-by-pulse basis. Instantaneous radar polarimetry enables detection based on full polarimetric properties of the target and hence can provide better discrimination against clutter. When compared to a radar system with a singly-polarized transmitter and a singly-polarized receiver instantaneous radar polarimetry can achieve the same detection performance (same false alarm and detection probabilities) with a substantially smaller transmit energy, or alternatively it can detect at substantially greater ranges for a given transmit energy. In

this section, we present the main idea for waveform transmission in IRP. The reader is referred to [14],[15] for simulation studies that demonstrate the value of IRP.

4.1. Unitary Waveform Matrices

Let us employ both polarization modes to transmit four phase-coded waveforms w_H^1, w_V^1, w_H^2, w_V^2. On each polarization mode we transmit two waveforms separated by a PRI T. We employ Alamouti coding [24] to coordinate the transmission of waveforms over the vertical (V) and horizontal (H) polarization channels; that is, we define

$$w_H^2 = \widetilde{w_V^1} \tag{31}$$

$$w_V^2 = -\widetilde{w_H^1}, \tag{32}$$

where $\tilde{\cdot}$ denotes complex conjugate time-reversal. After discretizing (at chip intervals) and converting time-indexed sequences to z-transform domain, we can write the radar receive equation in matrix form as

$$\mathbf{R}(z) = z^{-d}\mathbf{H}\mathbf{W}(z) + \mathbf{Z}(z) \tag{33}$$

where $\mathbf{R}(z)$ is the 2 by 2 radar measurement matrix at the receiver, $\mathbf{H}$ is the 2 by 2 scattering matrix in (30) and $\mathbf{Z}(z)$ is a noise matrix. The entries of $\mathbf{H}$ are taken to be constant since they correspond to a fixed range (delay d) and a fixed time. For now, we limit our analysis to zero-Doppler axis and will postpone the treatment of Doppler effect to Section 4.2. The Alamouti waveform matrix $\mathbf{W}(z)$ is given by

$$\mathbf{W}(z) = \begin{pmatrix} W_V^1(z) & -\widetilde{W}_H^1(z) \\ W_H^1(z) & \widetilde{W}_V^1(z) \end{pmatrix} \tag{34}$$

where $\widetilde{W}(z) = z^L \overline{W}(z^{-1})$ for a length L sequence w.

If we require the matrix $\mathbf{W}(z)$ to be unitary, that is,

$$\mathbf{W}(z)\widetilde{\mathbf{W}}(z) = \begin{pmatrix} W_V^1(z) & -\widetilde{W}_H^1(z) \\ W_H^1(z) & \widetilde{W}_V^1(z) \end{pmatrix} \begin{pmatrix} \widetilde{W}_V^1(z) & \widetilde{W}_H^1(z) \\ -W_H^1(z) & W_V^1(z) \end{pmatrix} = 2Lz^{-L} \begin{pmatrix} 1 & 0 \\ 0 & 1 \end{pmatrix} \tag{35}$$

then it is easy to estimate the scattering matrix $\mathbf{H}$ by post-multiplying (33) with $\widetilde{\mathbf{W}}(z)$. The unitary condition is equivalent to

$$|W_V^1(z)|^2 + |W_H^1(z)|^2 = 2L. \tag{36}$$

This is the same condition as the Golay complementary condition and is satisfied by choosing $W_V(z) = X(z)$ and $W_H(z) = Y(z)$, where $X(z)$ and $Y(z)$ are z-transforms of the Golay complementary sequences x and y, respectively. This shows that by properly coordinating the transmission of Golay complementary waveforms across polarizations and over time we can make the four channels HH, VV, VH, and HV available at the receiver (with delay L) using only linear processing. The four matched filters (in z-domain) are given by

$$\mathbf{Q}(z) = \begin{pmatrix} M_1(z)R_V(z) & M_2(z)R_V(z) \\ M_1(z)R_H(z) & M_2(z)R_H(z) \end{pmatrix} \tag{37}$$

where

$$M_1(z) = \widetilde{W}_V^1(z)z^{-L} - \widetilde{W}_H^1(z)$$
$$M_2(z) = \widetilde{W}_H^1(z)z^{-L} + \widetilde{W}_V^1(z). \tag{38}$$

and $R_V(z)$ denotes the first row of $\mathbf{R}(z)$ and represents the z-transform of the entire radar return (over two time slots) received on the vertical polarization channel.

Remark 1: The above description suggests that a radar image will be available only on every second pulse, since two PRIs are required to form an image. However, after the transmission of the first pulse, images can be made available at every PRI. This is done by reversing the roles of the waveforms transmitted on the two pulses. Thus, in the analysis, the matrix $\mathbf{W}(z)$ in (33) is replaced by

$$\mathbf{V}(z) = \begin{pmatrix} -\widetilde{W}_H^1(z) & W_V^1(z) \\ \widetilde{W}_V^1(z) & W_H^1(z) \end{pmatrix} \tag{39}$$

which is still unitary due to the interplay between Golay property and Alamouti coding. Moreover, the processing involved is essentially invariant from pulse to pulse: the return pulse in each of the and channels is correlated against the transmit pulse on that channel. This yields an estimate of the scattering matrix on each pulse.

4.2. Doppler Resilient IRP

In the previous section, we restricted our analysis to zero-Doppler axis. Off the zero-Doppler axis, a relative Doppler shift of θ exists between consecutive waveforms on each polarization channel and the radar measurement equation changes to

$$\mathbf{R}(z) = z^{-d}\mathbf{H}\mathbf{W}(z)\mathbf{D}(\theta) + \mathbf{Z}(z) \tag{40}$$

where $\mathbf{D}(\theta) = \text{diag}(1, e^{j\theta})$. Consequently, the unitary property of $\mathbf{W}(z)$ can no longer be used to estimate $\mathbf{H}$, due to the fact that $\mathbf{W}(z)\mathbf{D}(\theta)\widetilde{\mathbf{W}}(z)$ is not a factor of identity. In other words, off the zero-Doppler axis the four elements in $\mathbf{W}(z)\mathbf{D}(\theta)\widetilde{\mathbf{W}}(z)$ have range sidelobes.

The matrix $\mathbf{W}(z)\mathbf{D}(\theta)\widetilde{\mathbf{W}}(z)$ can be viewed as a *matrix-valued ambiguity function* (in z-domain) for IRP. In Section 3, we showed that the range sidelobes of the ambiguity function of a pulse train of Golay waveforms can be suppressed (in a desired Doppler band) by carefully selecting the order in which the Golay complementary waveforms are transmitted. This result can be extended to IRP. In fact, it is shown in [11] that the range sidelobes of the IRP matrix-valued ambiguity function can be cleared out along modest Doppler shifts by coordinating the transmission of the following Alamouti matrices

$$\mathbf{X}_1(z) = \begin{pmatrix} X(z) & -\widetilde{Y}(z) \\ Y(z) & \widetilde{X}(z) \end{pmatrix} \quad \text{and} \quad \mathbf{X}_{-1}(z) = \begin{pmatrix} -\widetilde{Y}(z) & -X(z) \\ \widetilde{X}(z) & -Y(z) \end{pmatrix} \tag{41}$$

according to the 1s and -1s in the PTM sequence, where 1 represents $\mathbf{X}_1(z)$ and -1 represents $\mathbf{X}_{-1}(z)$, and $X(z)$ and $Y(z)$ are z-transforms of the Golay pair (x, y).

Range sidelobes along higher Doppler intervals can be cleared out by coordinating the transmission of $\mathbf{X}_1(z)$ and $\mathbf{X}_{-1}(z)$ according to oversampled PTM pulse trains.

5. Conclusion

In this chapter, we focused on the use and control of degrees of freedom in the radar illumination pattern and presented examples to highlight the value of properly utilizing degrees of freedom. We showed that by coordinating the transmission of Golay complementary waveforms in time (or exploiting waveform agility over time) according to carefully designed biphase sequences we can construct pulse trains whose ambiguity functions have desired properties. We also showed that by combining Alamouti coding and Golay complementary property we can construct unitary polarization-time waveform matrices that make the full polarization scattering matrix of a target available for detection on a pulse-by-pulse basis. Looking to the future, we see unitary waveform matrices as a new illumination paradigm that enables broad waveform adaptability across time, space, frequency and polarization.

6. References

[1] M. I. Skolnik, "An introduction and overview of radar," in *Radar Handbook*, M. I. Skolnik, Ed. New York: McGraw-Hill, 2008.

[2] M. C. Wicks, M. Rangaswamy, R. Adve, and T. B. Hale, "Space-time adaptive processing," *IEEE Signal Processing Magazine*, no. 1, pp. 51–65, Jan. 2006.

[3] M. J. E. Golay, "Multislit spectrometry," *J. Opt. Soc. Am.*, vol. 39, p. 437, 1949.

[4] ——, "Static multislit spectrometry and its application to the panoramic display of infrared spectra," *J. Opt. Soc. Am.*, vol. 41, p. 468, 1951.

[5] ——, "Complementary series," *IRE Trans. Inform. Theory*, vol. 7, no. 2, pp. 82–87, April 1961.

[6] G. R. Welti, "Quaternary codes for pulsed radar," *IRE Trans. Inform. Theory*, vol. IT-6, no. 3, pp. 400–408, June 1960.

[7] M. R. Ducoff and B. W. Tietjen, "Pulse compression radar," in *Radar Handbook*, M. I. Skolnik, Ed. New York: McGraw-Hill, 2008.

[8] C. C. Tseng and C. L. Liu, "Complementary sets of sequences," *IEEE Trans. Inform. Theory*, vol. IT-18, no. 5, pp. 644–652, Sep. 1972.

[9] R. Sivaswami, "Multiphase complementary codes," *IEEE Trans. Inform. Theory*, vol. IT-24, no. 3, pp. 546–552, Sept. 1978.

[10] R. L. Frank, "Polyphase complementary codes," *IEEE Trans. Inform. Theory*, vol. IT-26, no. 6, pp. 641–647, Nov. 1980.

[11] A. Pezeshki, A. R. Calderbank, W. Moran, and S. D. Howard, "Doppler resilient Golay complementary waveforms," *IEEE Trans. Inform. Theory*, vol. 54, no. 9, pp. 4254–4266, Sep. 2008.

[12] ——, "Doppler resilient Golay complementary pairs for radar," in *Proc. Stat. Signal Proc. Workshop*, Madison, WI, Aug. 2007, pp. 483–487.

[13] S. Suvorova, S. D. Howard, W. Moran, R. Calderbank, and A. Pezeshki, "Doppler resilience, Reed-Muller codes, and complementary waveforms," in *Conf. Rec. Forty-first Asilomar Conf. Signals, Syst., Comput.*, Nov. 2007, pp. 1839–1843.

[14] S. D. Howard, A. R. Calderbank, and W. Moran, "A simple polarization diversity technique for radar detection," in *Proc. Second Int. Conf. Waveform Diversity and Design*, Lihue, HI, Jan. 2006.

[15] ——, "A simple signal processing architecture for instantaneous radar polarimetry," *IEEE Trans. Inform. Theory*, vol. 53, pp. 1282–1289, Apr. 2007.

[16] N. Levanon and E. Mozeson, *Radar Signals*. New York: Wiley, 2004.

[17] E. Prouhet, "Mèmoire sur quelques relations entre les puissances des nombres," *C. R. Acad. Sci. Paris Sèr.*, vol. I 33, p. 225, 1851.

[18] J. P. Allouche and J. Shallit, "The ubiquitous Prouhet-Thue-Morse sequence," in *Sequences and their applications, Proc. SETA'98*, T. H. C. Ding and H. Niederreiter, Eds. Springer Verlag, 1999, pp. 1–16.

[19] M. Morse, "Recurrent geodesics on a surface of negative curvature," *Trans. Amer. Math Soc.*, vol. 22, pp. 84–100, 1921.

[20] M. I. Skolnik, *Introduction to Radar Systems*, 3rd ed. McGraw-Hill, 2001.

[21] H. L. V. Trees, *Detection, Estimation and Modulation Theory, Part III*. New York: Wiley, 1971.

[22] R. K. Moore, "Ground echo," in *in Radar Handbook*, M. I. Skolnik, Ed. New York: McGraw-Hill, 2008.

[23] R. Sullivan, "Synthetic aperture radar," in *in Radar Handbook*, M. I. Skolnik, Ed. New York: McGraw-Hill, 2008.

[24] S. Alamouti, "A simple transmit diversity technique for wireless communications," *IEEE J. Select. Areas Commun.*, vol. 16, no. 8, pp. 1451–1458, Oct. 1998.